# π- and σ-Coordinated Al in AlC 2 - and AlCSi - . A Combined Photoelectron Spectroscopy and ab Initio Study

**ARTICLE** *in* JOURNAL OF THE AMERICAN CHEMICAL SOCIETY · NOVEMBER 1999

Impact Factor: 12.11 · DOI: 10.1021/ja992102z



**4 AUTHORS**, INCLUDING:

Alexander I Boldyrev
Utah State University
**341** PUBLICATIONS **9,969** CITATIONS
SEE PROFILE

Lai-Sheng Wang
Brown University
**464** PUBLICATIONS **19,888** CITATIONS
SEE PROFILE

# $\pi$- and $\sigma$-Coordinated Al in $AlC_2^-$ and $AlCSi^-$. A Combined Photoelectron Spectroscopy and ab Initio Study

**Alexander I. Boldyrev,*,†,‡ Jack Simons,*,† Xi Li,§ and Lai-Sheng Wang*,§**

*Contribution from the Department of Chemistry, The University of Utah, Salt Lake City, Utah 84112, Department of Chemistry and Biochemistry, Utah State University, Logan, Utah 84322-0300, Department of Physics, Washington State University, Richland, Washington 99352, and W. R. Wiley Environmental Molecular Sciences Laboratory, Pacific Northwest National Laboratory, MS K8-88, P.O. Box 999, Richland, Washington 99352*

*Received June 21, 1999*

**Abstract:** Vibrationally resolved photoelectron spectroscopy is combined with ab initio calculations to investigate the structure and chemical bonding in $AlC_2^-$ and $AlCSi^-$. $AlC_2^-$ was found to have a $C_{2v}$ structure whereas $AlCSi^-$ was found to be almost linear, thus establishing $\pi$-coordination of Al in $AlC_2^-$ and $\sigma$-coordination in $AlCSi^-$. The adiabatic electron affinities of $AlC_2$ and AlCSi were measured to be 2.65(3) and 2.50(6) eV, respectively. The calculated vertical (2.87 eV) and adiabatic (2.60 eV) electron detachment energies for $AlC_2^-$ agree well with the 2.73(0.03) and 2.65(0.03) eV experimental values, respectively. The calculated (2.86 eV) and experimental ($2.64 \pm 0.04$ eV) vertical detachment energies for $AlCSi^-$ were also in good agreement. The calculated vibrational frequency for $AlC_2$ and vertical detachment energies for other higher energy features in both $AlC_2^-$ and $AlCSi^-$ were also in good agreement with the experimental measurements. The combined experimental and theoretical effort allows us to elucidate the structures of $AlC_2^-$ and $AlCSi^-$ and the nature of their chemical bonding.

## Introduction

The −CC− group is known to bond to a variety of atoms and functional groups, such as H, F, and $CH_3$, using $\sigma$-coordination to produce linear X−C≡C−X neutral and X−C≡C$^-$ anion structures. However, when X is an electropositive atom such as Li, Mg, Al, Ti, etc., $\pi$-coordination is known to be more favorable.[1−8] Simple electrostatic models based on charge transfer from X to $C_2$ are used to explain why electropositive atoms prefer to form $\pi$-complexes. However, when one carbon atom is replaced by a more electropositive but isovalent atom such as silicon, it is not clear if the $\sigma$-complex of XCSi will be favored over the $\pi$-complex. In this work, we undertake a combined theoretical and experimental work on two anions $AlC_2^-$ and $AlCSi^-$ which help address the question of the relative stabilities of $\sigma$- and $\pi$-coordination of electropositive aluminum to $C_2^-$ and $CSi^-$. We found that indeed $\sigma$-coordination is favored in $AlCSi^-$, in contrast to $AlC_2^-$, where $\pi$-coordination occurs.

## Experimental Methods

We used anion photoelectron spectroscopy (PES) to obtain electronic and vibrational information about $AlC_2^-$, $AlCSi^-$, and their respective neutral species. The experiments were carried out with a magnetic-bottle time-of-flight PES apparatus, equipped with a laser vaporization cluster source. Details of the experiment have been described previously.[9,10] $AlC_2^-$ and $AlCSi^-$ were produced by laser vaporization of a graphite/Al or graphite/Al/Si composite target, respectively, with a pure helium carrier gas, and detected by a time-of-flight mass spectrometer. The anion species of interest were selected, decelerated, and photodetached with two photon energies: 355 (3.496 eV) and 266 nm (4.661 eV). Photoelectron time-of-flight spectra were measured and converted to electron binding energy spectra calibrated with the known spectrum of $Cu^-$. The electron kinetic energy resolution of the apparatus was typically 25 meV for 1 eV electrons.

## Computational Methods

We initially optimized the geometries of $AlC_2$, $AlC_2^-$, AlCSi, and $AlCSi^-$ employing analytical gradients with polarized split-valence basis sets (6-311+G*)[11−13] using the hybrid method, which includes a mixture of Hartree−Fock exchange with density functional exchange-correlation (B3LYP).[14−16] Then, the geometries were refined using the CCSD(T)

† The University of Utah.

‡ Utah State University.

§ Washington State University and Pacific Northwest National Laboratory.

(1) (a) Apeloig, Y.; Schleyer, P. v. R.; Binkley, J. S.; Pople, J. A.; Jorgenson, W. L. *Tetrahedron Lett*. **1976**, 3973. (b) Disch, R. L.; Schulman, J. M.; Ritchie, J. P. *J. Am. Chem. Soc*. **1984**, *106*, 6246. (c) Schleyer, P. v. R. *J. Phys. Chem*. **1990**, *94*, 5560.

(2) (a) Ramondo, F.; Bencivenni, L.; Grandinetti, F. *J. Mol. Struct. (THEOCHEM)* **1990**, *206*, 205. (b) Ramondo, N.; Sanna, F.; Bencivenni, L. *J. Mol. Struct. (THEOCHEM)* **1992**, *258*, 361.

(3) Green, S. *Chem. Phys. Lett*. **1984**, *112*, 29.

(4) Boldyrev, A. I.; Simons, J. *J. Phys. Chem. A* **1997**, *101*, 2215.

(5) Knight, L. B., Jr.; Cobranchi, S. T.; Herlong, J. O.; Arrington, C. A. *J. Chem. Phys*. **1990**, *92*, 5856.

(6) Flores, J. R.; Largo, A. *Chem. Phys*. **1990**, *140*, 19.

(7) Sumathi, R.; Hendrickx, M. *Chem. Phys. Lett*. **1998**, *287*, 496.

(8) Li, X.; Wang, L. S. *J. Chem. Phys*. Submitted for publication. Wang, X. B.; Ding, C. F.; Wang, L. S. *J. Phys. Chem. A* **1997**, *101*, 7699.

(9) Wang, L. S.; Cheng, H. S.; Fan, J. *J. Chem. Phys*. **1998**, *102*, 9480.

(10) Wang, L. S.; Wu, H. In *Advances in Metal and Semiconductor Clusters. IV. Cluster Materials*; Duncan, M. A., Ed.; JAI Press: Greenwich, 1998; pp 299−343

(11) McLean, A. D.; Chandler, G. S. *J. Chem. Phys*. **1980**, *72*, 5639.

(12) Clark, T.; Chandrasekhar, J.; Spitznagel, G. W.; Schleyer, P. v. R. *J. Comput. Chem*. **1983**, *4*, 294.

(13) Frisch, M. J.; Pople, J. A.; Binkley, J. S. *J. Chem. Phys*. **1984**, *80*, 3265.

(14) Parr, R. G.; Yang, W. *Density-functional theory of atoms and molecules*; Oxford University Press: Oxford, 1989.

(15) Becke, A. D. *J. Chem. Phys*. **1992**, *96*, 2155.

(16) Perdew, J. P.; Chevary, J. A.; Vosko, S. H.; Jackson, K. A.; Pederson, M. R.; Singh, D. J.; Fiolhais, C. *Phys. Rev. B* **1992**, *46*, 6671.

10.1021/ja992102z CCC: $18.00 
Published on Web 10/13/1999

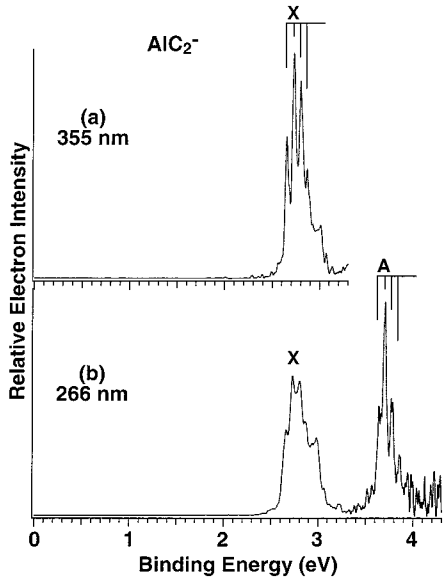


**Figure 1.** Photoelectron spectra of $AlC_2^-$ at (a) 355 nm (3.496 eV) and (b) 266 nm (4.661 eV). The observed detachment channels are labeled (X and A). Vertical lines indicate vibrational progressions.

method[17−19] and the same basis sets. Finally, the energies of the lowest-energy structures were refined using the CCSD(T) level of theory and the more extended 6-311+G(2df) basis sets. All core electrons were kept frozen in treating the electron correlation at the CCSD(T) levels of theory. Vertical electron detachment energies from the lowest-energy singlet structures of $AlC_2^-$ and $AlCSi^-$ were calculated using the outer valence Green function (OVGF) method[20−24] incorporated in Gaussian-94. The 6-311+G(2df) basis sets were used in all OVGF calculations, and all calculations were performed using the Gaussian-94 program.[25]

## Experimental Results

Figure 1 shows the PES spectra of $AlC_2^-$ at two wavelengths, 355 and 266 nm. The 355-nm spectrum revealed one band (X) that contains a well-resolved vibrational progression with a 590 $cm^{-1}$ spacing. The 0−0 transition yields an adiabatic electron affinity (ADE) of 2.65 eV for $AlC_2$ while the strongest vibrational feature yields a vertical detachment energy (VDE) of 2.73 eV. A second detachment feature (A) was observed at 3.71 eV VDE, also with a well-resolved vibrational progression of 590 $cm^{-1}$ spacing, similar to that in the X band.

Figure 2 displays the PES spectra of $AlCSi^-$ at the two detachment photon energies. The 355-nm spectrum shows two detachment features with VDEs at 2.64 (X) and 3.15 eV (A),

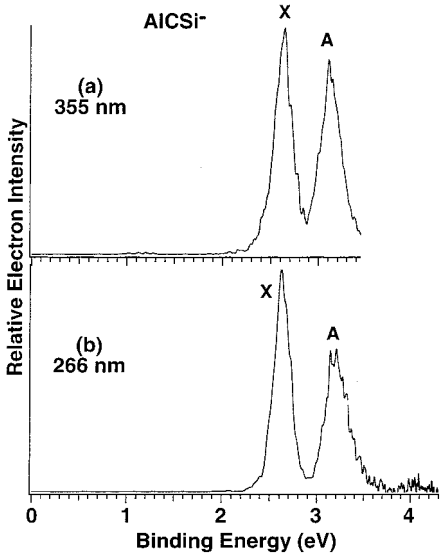


**Figure 2.** Photoelectron spectra of $AlCSi^-$ at (a) 355 nm (3.496 eV) and (b) 266 nm (4.661 eV). The observed detachment channels are labeled (X and A).

**Table 1.** Observed Adiabatic (ADE) and Vertical (VDE) Detachment Energies for $AlC_2^-$ and $AlCSi^-$ and the Obtained Spectroscopic Constants for $AlC_2$ and AlCSi

| | | ADE (eV) | VDE (eV) | term values (eV) | vib freq ($cm^{-1}$) |
|---|---|---|---|---|---|
| $AlC_2$ | X | 2.65(3) | 2.73(3) | 0 | 590(40) |
| | A | 3.63(4) | 3.71(4) | 0.98(4) | 590(50) |
| AlCSi | X | 2.50(6) | 2.64(4) | 0 | |
| | A | 3.02(8) | 3.15(6) | 0.52(8) | |

respectively. However, no vibrational structures were resolved for either band of the $AlCSi^-$ spectrum. The 266-nm spectrum of $AlCSi^-$ revealed no additional detachment features. The adiabatic electron affinity of AlCSi was estimated from the onset of the X feature to be 2.50 eV, which is slightly smaller than that for $AlC_2$.

The spectra of $AlC_2^-$ and $AlCSi^-$ are similar, except that the A-feature of $AlCSi^-$ has a considerably lower binding energy compared to that of the $AlC_2^-$ spectrum. The measured electron detachment energies and spectroscopic constants for $AlC_2$ and AlCSi are summarized in Table 1.

## Theoretical Results

**$AlC_2^-$.** At the B3LYP/6-311+G* level of theory, the global minimum of $AlC_2^-$ was found to have a linear singlet $C_{\infty v}$ ($^1\Sigma^+$, $1\sigma^2 2\sigma^2 1\pi^4 3\sigma^2 4\sigma^2$) structure (characterized in Table 2). The cyclic $C_{2v}$ ($^1A_1$, $1a_1^2 1b_2^2 2a_1^2 1b_1^2 3a_1^2 4a_1^2$) structure was found to be a local minimum only 1.4 kcal/mol higher in energy. However, at the higher CCSD(T)/6-311+G* level of theory, the $C_{\infty v}$ ($^1\Sigma^+$) linear structure is a second-order saddle point with the cyclic $C_{2v}$ ($^1A_1$) structure being the global minimum (Table 2). The linear structure corresponds to a barrier on the intramolecular rotation of $Al^+$ around the $C_2^{2-}$ group. The height of the internal rotation barrier is only 2.1 kcal/mol at the CCSD(T)/6-311+G(2df) level of theory.

**$AlC_2$.** At the B3LYP/6-311+G* level of theory, the global minimum of $AlC_2$ was found to have a cyclic $C_{2v}$ ($^2A_1$, $1a_1^2 1b_2^2 2a_1^2 1b_1^2 3a_1^2 4a_1^1$) structure (Table 2). A linear singlet $C_{\infty v}$ ($^2\Sigma^+$, $1\sigma^2 2\sigma^2 1\pi^4 3\sigma^2 4\sigma^1$) structure was found to be a local minimum, 8.7 kcal/mol higher in energy. At the CCSD(T)/6-311+G* level of theory, the $C_{\infty v}$ ($^1\Sigma^+$) linear structure becomes a second-order saddle point while the cyclic $C_{2v}$ ($^1A_1$)

(17) Cizek, J. *Adv. Chem. Phys*. **1969**, *14*, 35.
(18) Purvis, G. D., III; Bartlett, R. J. *J. Chem. Phys*. **1982**, *76*, 1910.
(19) Scuseria, G. E.; Janssen, C. L.; Schaefer, H. F., III *J. Chem. Phys*. **1988**, *89*, 7282.
(20) Cederbaum, L. S. *J. Phys*. **1975**, *B8*, 290.
(21) Niessen, W. von; Shirmer, J.; Cederbaum, L. S. *Comput. Phys. Rep*. **1984**, *1*, 57.
(22) Zakrzewski, V. G.; Niessen, W. von *J. Comput. Chem*. **1993**, *14*, 13.
(23) Zakrzewski, V. G.; Ortiz, J. V. *Int. J. Quantum Chem*. **1995**, *53*, 583.
(24) Ortiz, J. V.; Zakrzewski, V. G.; Dolgunitcheva, O. In *Conceptual Trends in Quantum Chemistry*; Kryachko, E. S., Ed.; Kluver: Dordrecht, 1997; Vol. 3, p 463.
(25) Frisch, M. J.; Trucks, G. W.; Schlegel, H. B.; Gill, P. M. W.; Johnson, B. G.; Robb, M. A.; Cheeseman, J. R.; Keith, T. A.; Peterson, G. A.; Montgomery, J. A.; Raghavachari, K.; Al-Laham, M. A.; Zakrzewski, V. G.; Ortiz, J. V.; Foresman, J. B.; Cioslowski, J.; Stefanov, B. B.; Nanayakkara, A.; Challacombe, M.; Peng, C. Y.; Ayala, P. Y.; Chen, W.; Wong, M. W.; Anders, J. L.; Replogle, E. S.; Gomperts, R.; Martin, R. L.; Fox, D. J.; Binkley, J. S.; DeFrees, D. J.; Baker, J.; Stewart, J. J. P.; Head-Gordon, M.; Gonzalez, C.; Pople J. A. *GAUSSIAN 94*, Revision A.1; Gaussian Inc.: Pittsburgh, PA, 1995.

**Table 2.** Calculated Molecular Properties of $AlC_2^-$ and $AlC_2$

| $AlC_2^-$, $C_{2v}$, $^1A_1$ | B3LYP/6-311+G* | CCSD(T)/6-311+G* | $AlC_2$ $C_{2v}$, $^2A_1$ | B3LYP/6-311+G* | CCSD(T)/6-311+G* |
|---|---|---|---|---|---|
| $R$(C−Al), Å | 2.034 | 2.030 | $R$(C−Al), Å | 1.943 | 1.943 |
| $R$(C−C), Å | 1.263 | 1.283 | $R$(C−C), Å | 1.265 | 1.287 |
| $E_{tot}$, au | −318.60875 | −317.93499 | $E_{tot}$, au | −318.51216 | −317.84560 |
| $\omega_1(a_1)$, $cm^{-1}$ | 1847 | 1770 | $\omega_1(a_1)$, $cm^{-1}$ | 1798 | 1718 |
| $\omega_2(a_1)$, $cm^{-1}$ | 579 | 595 $cm^{-1}$ | $\omega_2(a_1)$, $cm^{-1}$ | 615 | 623 |
| $\omega_3(b_2)$, $cm^{-1}$ | 105 | 129 $cm^{-1}$ | $\omega_3(b_2)$, $cm^{-1}$ | 355 | 395 |
| $AlC_2^-$, $C_{\infty v}$, $^1\Sigma^+$ | B3LYP/6-311+G* | CCSD(T)/6-311+G* | $AlC_2$, $C_{\infty v}$, $^2\Sigma^+$ | B3LYP/6-311+G* | CCSD(T)/6-311+G* |
| $R$(C−Al), Å | 1.874 | 1.876 | $R$(C−Al), Å | 1.884 | 2.024 |
| $R$(C−C), Å | 1.265 | 1.281 | $R$(C−C), Å | 1.250 | 1.247 |
| $E_{tot}$, au | −318.610935 | −317.93108 | $E_{tot}$, au | −318.49832 | −317.82726 |
| $\omega_1(\sigma)$, $cm^{-1}$ | 1922 | 1859 | $\omega_1(\sigma)$, $cm^{-1}$ | 1843 | 1974 |
| $\omega_2(\sigma)$, $cm^{-1}$ | 614 | 618 | $\omega_2(\sigma)$, $cm^{-1}$ | 509 | 623 |
| $\omega_3(\pi)$, $cm^{-1}$ | 114 | 145 i | $\omega_3(\pi)$, $cm^{-1}$ | 98 | 239 i |

**Table 3.** Calculated Molecular Properties of $AlCSi^-$ and AlCSi

| $AlCSi^-$, $C_{\infty v}$, $^1\Sigma^+$ | B3LYP/ 6-311+G* | CCSD(T)/ 6-311+G* | $AlCSi^-$, $C_s$, $^1A'$ | CCSD(T)/ 6-311+G* | AlCSi, $C_{\infty v}$, $^2\Sigma^+$ | B3LYP/ 6-311+G* | CCSD(T)/ 6-311+G* |
|---|---|---|---|---|---|---|---|
| $R$(C−Al), Å | 1.881 | 1.883 | $R$(C−Al), Å | 1.883 | $R$(C−Al), Å | 1.822 | 1.830 |
| $R$(C−Si), Å | 1.680 | 1.693 | $R$(C−Si), Å | 1.694 | $R$(C−Si), Å | 1.672 | 1.682 |
| ∠AlCSi, deg | 180.0 | 180.0 | ∠AlCSi, deg | 160.1 | ∠AlCSi, deg | 180.0 | 180.0 |
| $E_{tot}$, au | −570.04215 | −568.97738 | $E_{tot}$, au | −568.97759 | $E_{tot}$, au | −569.94758 | −568.88825 |
| $\omega_1(\sigma)$, $cm^{-1}$ | 1258 | 1239 | $\omega_1(a')$, $cm^{-1}$ | 1223 | $\omega_1(\sigma)$, $cm^{-1}$ | 1251 | 1257 |
| $\omega_2(\sigma)$, $cm^{-1}$ | 485 | 485 | $\omega_2(a')$, $cm^{-1}$ | 514 | $\omega_2(\sigma)$, $cm^{-1}$ | 509 | 509 |
| $\omega_3(\pi)$, $cm^{-1}$ | 91 | 93 i | $\omega_3(a')$, $cm^{-1}$ | 74 | $\omega_3(\pi)$, $cm^{-1}$ | 63 | 100 i |

structure remains the global minimum (Table 2). This structure was also found to be the global minimum in previous ab initio calculations[5,6] as was established experimentally.[5] The linear structure represents a barrier on the intramolecular rotation $Al^+$ around the $C_2^-$ group. The height of the internal rotation barrier is 12.3 kcal/mol at the CCSD(T)/6-311+G(2df) level of theory.

The calculated vertical and adiabatic electron detachment energies for $AlC_2^-$ were found to be the following: VDE = 2.87 eV (OVGF/6-311+G(2df)) and ADE = 2.60 eV (CCSD(T)/6-311+G(2df)). Both $AlC_2^-$ and $AlC_2$ are very stable thermodynamically with dissociation energies calculated to be the following: $\Delta E$ = 4.52 eV for $AlC_2^-$ ($C_{2v}$, $^1A_1$) → $C_2^-$ ($D_{\infty h}$, $^2\Sigma_g^+$) + Al ($^2P$) and $\Delta E$ = 5.06 eV for $AlC_2$ ($C_{2v}$, $^2A_1$) → $C_2$ ($D_{\infty h}$, $^1\Sigma_g^+$) + Al ($^2P$) (all at the CCSD(T)/6-311+G(2df) level of theory).

**$AlCSi^-$.** At the B3LYP/6-311+G* level of theory, the global minimum of $AlCSi^-$ was found to have a linear singlet $C_{\infty v}$ ($^1\Sigma^+$, $1\sigma^2 2\sigma^2 3\sigma^2 1\pi^4 4\sigma^2$) structure (characterized in Table 3). Alternative linear singlet $AlSiC^-$ $C_{\infty v}$ ($^1\Sigma^+$, $1\sigma^2 2\sigma^2 3\sigma^2 1\pi^4 4\sigma^2$) structure was also optimized at the B3LYP/6-311+G* level of theory, and it was found to be a second-order saddle point 60.8 kcal/mol higher in energy than the global minimum and it was excluded from further examination. The cyclic $C_s$ ($^1A'$, $1a'^2 2a'^2 3a'^2 4a'^2 1a''^2 5a'^2$) structure collapsed into the $AlCSi^-$ $C_{\infty v}$ ($^1\Sigma^+$) structure upon geometry optimization. However, at the CCSD(T)/6-311+G* level of theory, the $C_{\infty v}$ ($^1\Sigma^+$) linear structure becomes a second-order saddle point, and a bent $C_s$ ($^1A'$) structure becomes the global minimum (Table 3). The bent structure of $AlCSi^-$ is very different from the global minimum cyclic structure of $AlC_2^-$ because it does not have a Al−Si bond and the AlCSi angle is 160° compared to the AlCC angle of 72° in $AlC_2^-$. A similar bent structure was found to be the global minimum for the isoelectronic neutral molecule SiCSi.[26−31] The energy required for linearization of $AlCSi^-$ is only 0.132 kcal/mol, which is comparable to the difference in ZPE corrections (0.124 kcal/mol) between the linear and bent structures (all at the CCSD(T)/6-311+G* level of theory). Therefore, $AlCSi^-$ has a nearly linear equilibrium structure, especially when zero-point vibrational motion is considered.

The $AlCSi^-$ anion is also very stable toward dissociation. The dissociation energy was calculated to be $\Delta E$ = 4.26 eV for $AlCSi^-$ ($C_{2v}$, $^1A_1$) → $CSi^-$ ($C_{\infty v}$, $^2\Sigma^+$) + Al ($^2P$) (at the CCSD(T)/6-311+G(2df) level of theory).

**AlCSi.** At the B3LYP/6-311+G* level of theory, the global minimum of AlCSi was found to have a linear doublet $C_{\infty v}$ ($^2\Sigma^+$, $1\sigma^2 2\sigma^2 3\sigma^2 1\pi^4 4\sigma^1$) structure, but this becomes a second-order saddle point at the CCSD(T)/6-311+G* level of theory. According to Koopmans' theorem, the $1\pi$-MO is very close in energy to the $4\sigma$-HOMO in $AlCSi^-$. Therefore we also optimized the geometry of another linear doublet $C_{\infty v}$ ($^2\Pi'$, $1\sigma^2 2\sigma^2 3\sigma^2 1\pi^3 4\sigma^2$) structure at the CCSD(T)/6-311+G* level of theory. This state was found to be linear, but 0.25 eV higher in energy than the $C_{\infty v}$ ($^2\Sigma^+$, $1\sigma^2 2\sigma^2 3\sigma^2 1\pi^4 4\sigma^1$) linear structure (Table 3) and therefore not the global minimum for AlCSi. Unfortunately, because the two $C_{\infty v}$ ($^2\Sigma^+$, $1\sigma^2 2\sigma^2 3\sigma^2 1\pi^4 4\sigma^1$) and $C_{\infty v}$ ($^2\Pi'$, $1\sigma^2 2\sigma^2 3\sigma^2 1\pi^3 4\sigma^2$) states are so close in energy, we were not able to complete the geometry optimization at the CCSD(T)/6-311+G* level of theory at bent geometries due to convergence problems. We therefore were unable to calculate the adiabatic electron detachment energy of $AlCSi^-$.

In all four species studied here, the B3LYP method predicted a minimum in the linear configuration that is not preserved in the CCSD(T) calculations. We believe that the artificial minima for the linear configuration are essentially due to the one-configurational nature of the B3LYP method. One needs to use methods beyond the one-configurational approximation, such as CCSD(T) used here, to get reliable results for the species studied here.

(26) Weltner, E., Jr.; Mcleod, D., Jr. *J. Chem. Phys.* **1964**, *41*, 235.
(27) Kafafi, Z. H.; Hauge, R. H.; Fredin, L.; Margrave, J. L. *J. Phys. Chem.* **1983**, *87*, 797.
(28) Presilla-Marquez, J. D.; Graham, W. R. M. *J. Chem. Phys.* **1991**, *95*, 5612.
(29) Grev, R. S.; Schaefer, H. F., III *J. Chem. Phys.* **1985**, *82*, 4126.
(30) Rittby, C. M. L. *J. Chem. Phys.* **1991**, *95*, 5609.
(31) Bolton, E. E.; DeLeeuw, B. J.; Fowler, J. E.; Grev, R. S.; Schaefer, H. F., III *J. Chem. Phys.* **1992**, *97*, 5586.

**Table 4.** Comparison of Calculated and Experimental Electron Detachment Processes of $AlC_2^-$

| $C_{2v}$, $^1A_1$ state | expt VDE (eV) | expt ADE (eV) | electron detachment from MO | theory VDE[a] (eV) | theory, ADE[b] (eV) | $C_{\infty v}$, $^1\Sigma^+$ state | electron detachment from MO | theory VDE[a] (eV) |
|---|---|---|---|---|---|---|---|---|
| X | 2.73(3) | 2.65(3) | $4a_1$ | 2.87(0.90) | 2.60 | X | $4\sigma$ | 3.54(0.89) |
| A | 3.71(4) | 3.63(4) | $3a_1$ | 3.64(0.87) | | A | $1\pi$ | 3.99(0.88) |

[a] Pole strength is given in parentheses. [b] At the CCSD(T)/6-311+G(2df) level of theory using CCSD(T)/6-311+G* geometry.

**Table 5.** Comparison of Calculated and Experimental Vertical Electron Detachment Energies (VDE) of $AlCSI^-$

| $C_s$, $^1A'$ state | exptl VDE (eV) | electron detachment from MO | theory VDE[a] (eV) |
|---|---|---|---|
| X | 2.64(4) | 5a′ | 2.86(0.88) |
| A | 3.15(6) | 1a″ | 3.01(0.88) |
| | | 4a′ | 3.00(0.88) |

## Interpretation of the Experimental Spectra

**$AlC_2^-$.** In Table 4 we present the results of our calculations of the two major low-lying vertical one-electron detachment processes from the cyclic $C_{2v}$ ($^1A_1$) state of $AlC_2^-$.

**Feature X.** The lowest vertical electron detachment occurs by electron removal from the $4a_1$-HOMO. The feature X (Figure 1) peaking at $2.73 \pm 0.03$ eV agrees well with the calculated VDE of 2.87 eV [OVGF/6-311+G(2df)] from the $4a_1$-HOMO. The 355-nm spectrum revealed a well-resolved vibrational progression with a 590-$cm^{-1}$ spacing. According to our calculations, the main change in geometry upon electron detachment of $AlC_2^-$ occurs in the Al−C distance, which is 0.087 Å shorter in the neutral $AlC_2$. Therefore, one expects a vibrational progression due to the Al−$C_2$ stretching mode in the PES spectrum of $AlC_2^-$. The calculated value for the frequency of this vibration ($\nu_2$ in Table 2) is in good agreement with the experimentally observed vibrational spacing of 590 $cm^{-1}$, considering the large uncertainty of the measured value. The 0−0 transition yields an adiabatic electron affinity of 2.65 eV for $AlC_2$ that again agrees well with the calculated value of 2.60 eV (CCSD(T)/6-311+G(2df)).

**Feature A.** The second vertical electron detachment from the $3a_1$-(HOMO-1) should occur at 3.64 eV (OVGF/6-311+G(2df)) (Table 4). This value agrees well with the second detachment feature (A), which was observed at 3.71 eV. Unfortunately, the CCSD(T) method is not suitable for calculations of excited states having the same symmetry as the lower states, so we were not able to calculate the geometry relaxation and frequencies for the first excited state of $AlC_2$. We were able to calculate the vertical detachment energy because of the OVGF method used.

In Table 4 we also present the calculated electron detachment energies for the linear $AlC_2^-$ $C_{\infty v}$ ($^1\Sigma^+$, $1\sigma^2 2\ \sigma^2 1\pi^4 3\sigma^2 4\sigma^2$). It is clear that these VDEs do not agree nearly as well with the experimental PES spectra. We therefore conclude that both $AlC_2^-$ and $AlC_2$ have the cyclic $C_{2v}$ structures based on our calculations and experimental data.

**$AlCSi^-$.** In Table 5 we present the results of our calculations of the two major low-lying vertical one-electron detachment processes from the slightly bent $C_s$ ($^1A'$) state of $AlCSi^-$.

**Feature X.** The lowest vertical electron detachment occurs by electron removal from the 5a′-HOMO. The feature X (Figure 1) peaking at $2.64 \pm 0.04$ eV is in reasonable agreement with the calculated VDE of 2.86 eV [OVGF/6-311+G(2df)] from the 5a′-HOMO. There were discernible vibrational structures in the X-feature, which was probably due to the C−Al stretching. However, the bending mode, which has a very low frequency (Table 3), was probably also active, resulting in the broad and unresolved feature.

**Feature A.** The second vertical electron detachment from the very closely spaced 1a″-MO or 4a′-MO (which are almost degenerate because they originate from the $1\pi$-HOMO in the linear structure) occurs at 3.01 eV (OVGF/6-311+G(2df)). This value agrees well with the second detachment feature (A), observed at $3.15 \pm 0.06$ eV. The 266-nm spectrum revealed a splitting in the second peak, which might derive from the quasidegeneracy of the 1a″ and 4a′ MO found in our calculations. We therefore conclude that both $AlCSi^-$ and AlCSi have quasilinear structures based on our calculations and the experimental data.

## Discussion

The overall agreement between the experimental PES spectra and the theoretical calculations is quite satisfying. In particular, the excellent agreement between the calculations and the experimentally observed peak X in $AlC_2^-$ provides strong support for the cyclic structure with $\pi$-coordination of aluminum to $C_2$ in $AlC_2^-$ and in $AlC_2$. The cyclic structure of $AlC_2$ was previously found in ab initio calculations[5,6] and in rare gas matrix electron spin resonance studies by Knight and others.[5]

The agreement between the calculations and observed PES spectral features of the $AlCSi^-$ anion provides strong support for the quasilinear structure with $\sigma$-coordination of aluminum in $AlCSi^-$ and in AlCSi. The vertical and adiabatic electron detachment energies are also very high for the $AlCSi^-$ anion (Table 1) and they can be explained in the same fashion as in the $AlC_2^-$ anion. Surprisingly, both VDE and ADE of $AlCSi^-$ are very close to the corresponding values in $AlC_2^-$, despite the fact that one carbon was substituted by a more electropositive silicon atom. On the other hand, one should take into account the fact that $AlCSi^-$ has $\sigma$-coordination, while $AlC_2^-$ has $\pi$-coordination. If we compare the $\sigma$-complexes for both anions, $VDE(AlC_2^-) = 3.54$ eV and $VDE(AlCSi^-) = 2.86$ eV, one can see a substantial reduction in electron binding energy in $AlCSi^-$. Simple electrostatic considerations can also help to understand why $AlC_2^-$ has $\pi$-complex structure, while $AlCSi^-$ has $\sigma$-complex structure. Although the effective atomic charges in both anions show a high degree of ionicity, the two carbon atoms have the same charges in the cyclic $AlC_2^-$, whereas in $AlCSi^-$ the carbon carries a larger negative charge than silicon, which favors the $\sigma$-complex configuration in the latter.

## Conclusions

We report a combined experimental and theoretical investigation of $AlC_2^-$ and $AlCSi^-$ and their corresponding neutrals. Photoelectron spectra of the anions were measured and the electron detachment energies and vibrational frequencies were obtained. The adiabatic electron affinities of $AlC_2$ and AlCSi were determined to be 2.65(3) and 2.50(6) eV, respectively. The first electronic excited state was also observed for each species. Our theoretical calculations predicted that $AlC_2^-$ and $AlC_2$ both have a $C_{2v}$ cyclic structure while $AlCSi^-$ and AlCSi have quasilinear structures. The agreement between the calcu-

lated and experimental spectroscopic parameters confirms the $\pi$-coordination of Al in $AlC_2^-$ and $\sigma$-coordination of Al in $AlCSi^-$.

**Acknowledgment.** The theoretical work done in Utah is supported by the National Science Foundation (CHE-9618904). The authors acknowledge the Center for High Performance Computations at the University of Utah for computer time. The experimental work done in Washington is supported by the National Science Foundation (DMR-9622733). The experiment was performed at the W. R. Wiley Environmental Molecular Sciences Laboratory, a national scientific user facility sponsored by DOE's Office of Biological and Environmental Research and located at Pacific Northwest National Laboratory, which is operated for DOE by Battelle under Contract DE-AC06-76RLO 1830. L.S.W. is an Alfred P. Sloan Foundation Research Fellow.

JA992102Z